Casting of complex structures in aluminum using gypsum molds produced via binder jetting

Luca Giorleo and Michele Bonaventi
University of Brescia, Brescia, Italy

Abstract

Purpose – The purpose of present paper is to enlarge the knowledge about the performance of gypsum powder to realize complex molds or cores for aluminum casting.

Design/methodology/approach – The research was divided into two activities: simple; and complex-part production capability. In the simple-part step, the performance of gypsum powder and the minimum mold thickness that would withstand the casting process. In the complex-part step, the authors first investigated the powder removability as a function of geometry complexity and then binder jetting performance was evaluated for the case of lattice-structure fabrication.

Findings – All the geometries tested withstand the casting process demonstrating the benefits in terms of complexity part design; however, the process suffers of all the typical defect of casting as misrun, porosity and cold shut.

Originality/value – The results found in this research improve the benefits related to additive manufacturing application in industrial environment and in particular to the binder jetting technology and the rapid casting approach.

Keywords Binder jetting, Lattice structure, Mold casting, Expandable mold casting

Paper type Research paper

1. Introduction

Additive manufacturing (AM) technologies produce parts based on the layering approach; hence, the 3D complexity of a part is reduced to a summation of simpler 2D parts (Kyogoku, 2018). Therefore, the complexity of a part has virtually no limits. The capabilities of AM design can be summarized in the following four categories: shape complexity; hierarchical complexity; functional complexity; and material complexity. An important innovation in product design is the possibility to use topology optimization software to generate new geometries to increase product performance or decrease product weight. Based on this potential various industries, such as the aeronautical, automotive and the medical, have been leaning toward the application of AM to produce innovative metal products.

At present, the most developed metal AM process is powder bed fusion (PBF), which uses thermal energy to selectively melt and fuse material powder together. PBF can generate highly accurate parts and can be used for the direct manufacturing of end-use products (Bahnini *et al.*, 2018; Pham and Gault, 1998; Dickens, 1995). The negative aspects of this process are mainly the following:

- Narrow range of materials: the machine cannot function with all materials because the powder must be prepared carefully and the laser must be able to sinter it.
- Support structure: because are composed of the same part material can be difficult to eliminate. Moreover, a direct correlation between part complexity and volume of the support structure exists, which is a constraint to the part design.
- Part size: the available printable volume is still limited to small/medium dimensions within the range of centimeters; meanwhile, the production time is sufficiently high to be considered more expensive than the traditional ones.

To overcome the limits of PBF process, the performance of other AM technologies, such as binder jetting, has started being tested in the production of metal parts (Lores *et al.*, 2019; Ziaee and Crane, 2019).

The current issue and full text archive of this journal is available on Emerald Insight at: **https://www.emerald.com/insight/1355-2546.htm**

Rapid Prototyping Journal
27/11 (2021) 13–23
Emerald Publishing Limited [ISSN 1355-2546]
[DOI 10.1108/RPJ-03-2020-0048]

The authors gratefully thank Fondital S.p.a and, particularly, Silvio Tiboni and Mattia Cominelli for the essential support during the entire work.

Received 6 March 2020
Revised 13 July 2020
16 December 2020
12 April 2021
Accepted 12 May 2021

1.1 State of art

In binder jetting process, two materials are used: a powder-based material and a binder; the binder acts as an adhesive between powder layers. Binder jetting technology has the advantage of being a cold process and does not require support structures. Over the past few years, binder jetting has been tested for the direct fabrication of metal parts using polymeric, metal particle suspension, metal salts, or metal organic composition as a binder (Bai and Williams, 2018). After having been printed, the product is sintered to improve its mechanical properties. So it is possible to fabricate parts out of bronze (Bai and Williams, 2015), ceramic materials (Gonzalez *et al.*, 2016), stainless steel (Huang *et al.*, 2017) and titanium (Sheydaeian and Toyserkani, 2018) among others. However, the available materials that must be gas atomized are still limited. Typically, polymer de-binding requires a refined sintering profile to facilitate polymer pyrolysis and degassing. The pyrolysis of the polymer binder may lead to residual carbon, which could affect the purity (hence, the mechanical, optical and electrical/thermal properties) of the final part (Lores *et al.*, 2019). A different approach would be to use binder jetting technology to produce molds for sand casting to attempt the fabrication of complex geometries and intricate cavities, which are either too expensive (Almaghariz *et al.*, 2016) or impossible to realize (Chhabra and Singh, 2011; Druschitz *et al.*, 2014) with the traditional mold-fabrication process. In fact, it is not necessary to use a pattern (Lynch *et al.*, 2017) to obtain the "negative" of the part that will be realized at the end of the process; therefore, problems related to the cavities, undercuts, drafted angles and partition lines can be overcome. In addition, cores and molds are created simultaneously getting less costly than the common process (Kang and Ma, 2017). Therefore, an almost near-net-shape casting can be realized. Moreover, rapid tooling is important to the industries (Rooks, 2002) in terms of reducing prototyping cost. Today, the main companies who positioned themselves in the market of additively manufactured sand molds are Voxeljet, ExOne (Le Néel *et al.*, 2018a) and various research works are available that are focused on binder jetting applications in sand casting using these printers (Zhao *et al.*, 2018; Le Néel *et al.*, 2018b). The available research studies have been focused on the influence of the following process parameters (Hodder and Chalaturnyk, 2019): analysis of the cast dimensional accuracy pouring aluminum alloys (Le Néel *et al.*, 2018b); measuring the influence of the part/wall thickness on the part cooling time (Walker *et al.*, 2018); leverages binder jetting technology to design a smart molds with sensor integrated to study the thermodynamics and physics of the casting process (Szymański and Borowiak, 2019); testing the effect of different sand graininess and different binder on the casted part roughness. Furthermore, several studies have been conducted on the generation of complex molds via the use of 3D printing: cellular structures have been designed to obtain complex aluminum (Snelling *et al.*, 2015; Kim *et al.*, 2018) and iron casts (Wang *et al.*, 2019; Druschitz *et al.*, 2017) or lattice-reinforced thickness-varying shell molds (Shangguan *et al.*, 2018; Shangguan *et al.*, 2017).

1.2 Research objectives

However, despite the benefits of using silica sand, certain application limits still exist. The main problem is that the binder is a furan resin; hence, a mechanical process dedicated to destroying molds should be designed. This post-process could be critical when the part complexity is high because residuals of certain materials could remain within the inner regions. A solution would be the creation of molds using plaster powder that would be able to withstand high temperatures and, at the same time, would be water-soluble. In literature preliminary researches are available where direct metallic cast in plaster mold were successfully tested in case of simple geometries (Garzón *et al.*, 2017) or as a function of different heat treatment post process (Rodríguez-González *et al.*, 2020). Based on the aforementioned possible solution, to enlarge the knowledge about this topic the authors tested the performance of gypsum powder to realize complex molds or cores for aluminum casting. First, the gypsum resistance at casting temperature was tested. Then, different experimental campaigns were designed to test gypsum performance as a function of the wall thickness and the cast complexity. About cast complexity, it was investigated both binder jetting capability to produce the molds and part quality that is possible to obtain.

2. Materials and methods

The research was divided into two activities: simple and complex-part production capability. In the simple-part step, the performance of gypsum powder at casting temperature was tested (SP.1). Based on the performance results, open cubic molds were fabricated to test the minimum mold thickness that would withstand the casting process (SP.2). In the complex-part step, the authors first investigated the powder removability as a function of geometry complexity (CP.1); then, binder jetting performance was evaluated for the case of lattice-structure fabrication (CP.2). Table 1 summarizes the research workflow.

The 3D System Project 460 Plus was used for part fabrication. Calcium sulfate hemihydrate powder (Table 2) was used to produce the casting molds. The binder used in the printer was 2-Pyrrolidone; Table 2 lists the powder and binder properties. The

Table 1 Research workflow

Activities	Sub activities	Sample design	Analysis
Simple part (SP)	SP.1 Powder characterization	Cube	Temperature test
	SP.2 Simple-part production	Open cubic molds	Mold integrity Cast defects Surface Roughness
Complex part (CP)	CP.1 Binder Jetting design limit	Block parts with internal 2 D/3D complex channel	Powder removability
	CP.2 Complex-part production	Lattice structure	Mold integrity Cast defects

Table 2 Powder and binder properties

Chemical name	Melting point [°C]	Density [g/cm^3]	Powder size diameter [μm] (Farzadi *et al.*, 2014)	Water solubility [20°C in g/l]
Calcium sulfate hemihydrate	1,450	2.6–2.7	27	0.83% (3°C)
2-Pyrrolidone	100	1	Liquid	Not declared

aluminum alloy cast during the aforementioned tests was GMW5 and its base chemical composition was (Al) Si9Cu3Fe1 (Table 3). A gravity casting process was performed for the SP.2 and CP.2 steps at a temperature of 720°C.

The process parameters and the methods adopted for each step will be reported next.

2.1 Simple-part activity

For the powder characterization (SP.1), two sets of cubes with seven different dimensions (from 5 to 35 mm) were designed (Figure 1). A temperature test was conducted at 720°C, which corresponds to the casting aluminum temperature. The first set of cubes was left in a muffle furnace for 10 min and the second set for 15 min. The maintenance time was selected according to the aluminum solidification time. Finally, a qualitative analysis of the samples was performed to confirm whether the parts withstood the temperature. In SP.2, to test the minimum mold size, seven simple molds with an open cubic design (length 60 mm) and a wall thickness between 5 and 35 mm were fabricated (Figure 2). The samples were left in an oven for 12 h at 50°C to eliminate humidity prior to pouring the metal. Next, a qualitative and dimensional analysis of the obtained casts was performed to examine the inner porosity. Finally, five measures of surface roughness have been randomly executed on the sample bottom and sides with the Mitutoyo Surftest SJ-400.

2.2 Complex-part activity

The complex part activity was designed to study the complexity limits of a mold produced by binder jetting technology. In particular to produce mold with internal complex cavities could generate a problem related to possible restriction in removing the powder that acts as support structure. To test binder jetting post-process ability to discharge the unbound powder from hollow parts (CP.1 step), different molds with internal channels having a circular cross section were designed. The channel shape and orientation (2 D/3D) were varied; moreover, the cross-section diameters (5, 7.5 and 10 mm) were studied. Figure 3 presents the geometries generated for the test.

The geometries illustrated in Figure 3 were used for the Boolean subtractive function to generate 24 molds (4 shapes, 3 diameters, 2 orientations) with internal complex channel geometries. The powder removal ability was tested with a pressure gun at 8 bar.

The lattice geometries selected as demonstrators of the CP.2 are Diamond and Schwarz P. Figure 4 reports the selected geometries and the related design parameters as cell length (X), cell width (Y), cell height (Z), Diamond node diameter (Dn), Diamond node connector (Dc) and Schwarz P width (W).

Table 4 Lattice parameter design

Geometry	Cell dimension [mm]	Node thickness [mm]
Diamond (D) – Schwarz P (S)	60–30	5–7.5

Figure 1 Two sets of cubes tested for the SP.1

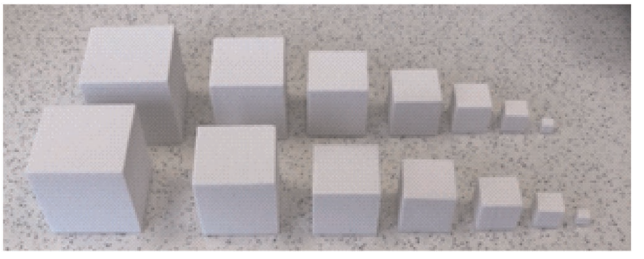

Figure 2 Open molds used for the SP.2

In this sub activity, a cubic lattice cell with equal length width and height have been considered for both geometries and reported as cell dimension; the parameter Dn, Dc and W have been equal and reported as node thickness. The cubic design space with a length equal to 60 mm was selected coherent with SP.2. Based on the aforementioned assumptions eight samples with an internal complexity generated by the lattice structure were designed as a function of shape (Diamond and Schwarz P), cell dimension (30 and 60 mm) and node-thickness (5 and 7.5 mm). Table 5 summarizes the different geometry parameters.

Figure 5 presents the lattice structure obtained by varying the parameters listed in Table 3. For clarity, each sample is indexed

Table 3 Chemical composition analysis of the aluminum alloy cast during the test

Element	Al	Cu	Mg	Si	Fe	Mn	Ni	Zn	Other
Percentage [%]	86.93	2.111	0.172	8.389	0.849	0.229	0.079	0.963	0.278

Figure 3 Complex internal channel design

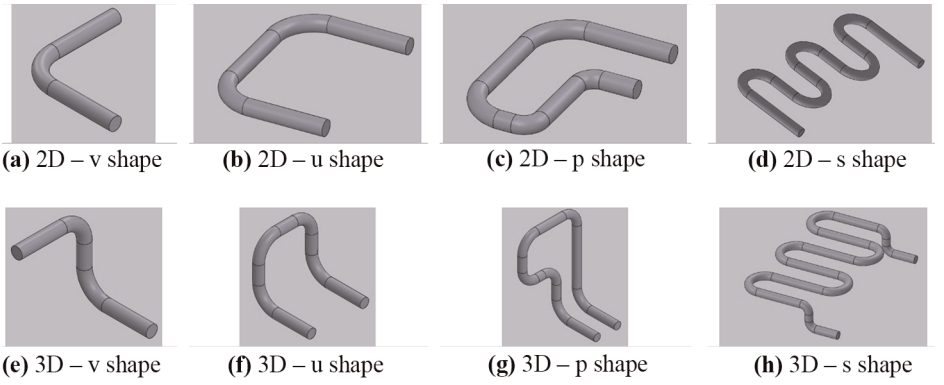

Figure 4 Demonstrators design for CP.2

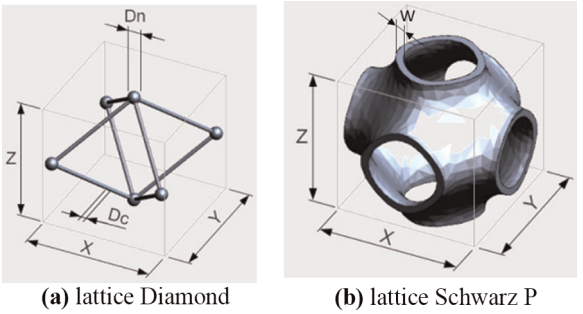

(a) lattice Diamond **(b)** lattice Schwarz P

with a code that classifies the geometry as a function of shape, cell dimension and cell thickness.

The geometries shown in Figure 5 were used to design the internal cavity of a close mold. More specifically, each geometry was used to generate the full (core) or the void (cast) part of a mold in a manner that 16 molds could be produced; a bottom gating system was added as well. Figures 6 illustrate core (CO) and cast (CA) negative design of the molds generated with node thickness equal to 5 mm; molds with 7.5 mm node thickness will have same design.

As illustrated in Figure 6 the gating system has a pouring basin with a conical shape and a sprue directly connected with the side surface of the part. For all the core geometries the gate is located in the bottom; in the diamond cast geometries the gate location is in correspondence of the lower node for D_CA_30_5 and in the middle still on the node for the D_CA_60_5. About the Schwarz P cast part the gate is located on the lower part of the external boundary cylinder.

After the molds production, a burnout cycle was executed to reduce defects caused by gas generation that occurs when binders are exposed to the high temperatures of molten metal. The burnout temperature and time depend on the binder chemical composition and melting point (Snelling *et al.*, 2014; Mckenna *et al.*, 2008): determined that the best permeability occurred when the molds were baked at 227°C for 6.2 h and the best compressive strength at 173°C for 5.5 h using binder resin; in case of furan resin (Mitra *et al.*, 2019) suggests a curing process of 100°C for 2 h. In this research because of the low melting point of binder and thin dimension of the designed parts, all molds had been pretreated in a furnace for 15 min at 150°C.

Finally, molten aluminum was melted in the fabricated molds to test their performance; the gravity-casting process parameters were selected according to SP.2. A maintenance time of 10 min was set to check the integrity of the molds against the molten aluminum temperature. Next, the expandable ability of the molds was tested by performing mold immersion in a water bath for 10 min. A defect analysis was performed to evaluate the quality of the casts.

Table 5 resumes the geometries and experiments designed for all campaigns.

To better understand the mechanism that occurs during filling and solidification the casting process was simulated with Inspire Cast software. Coherent with the experimental an inlet virtual gate having circular geometry with a 7.5 mm radius was set. For the casting process parameter, a spoon height approach was set because a totally manual ladle operators have been executed. Spoon height H is the distance between the ladle and the mold when the liquid is being poured and its relation with

Table 5 Experimental design for all the campaigns

Campaign	Geometry tested	Experiments
SP.1	7 cubes with length equal to 5, 10, 15, 20, 25, 30, 35 mm	2 oven treatment: 10 min at 720°C and 15 min at 720°C
SP.2	7 open cubic molds (length 60 mm) with wall thickness equal to 5, 10, 15, 20, 25, 30, 35 mm	Aluminum casting at 720°C
CP.1	24 molds with internal complex shape (4 shapes, 3 diameters, 2 orientations)	Remove unbound powder with a pressure gun at 8 bar
CP.2	16 complex mold as a function of their geometry (Diamond; Schwarz P), cell dimension (60, 30 mm), node thickness (5, 7.5 mm) and function (cast; core)	Aluminum casting at 720°C

Figure 5 Lattice structure samples as a function of shape – cell dimension – node thickness

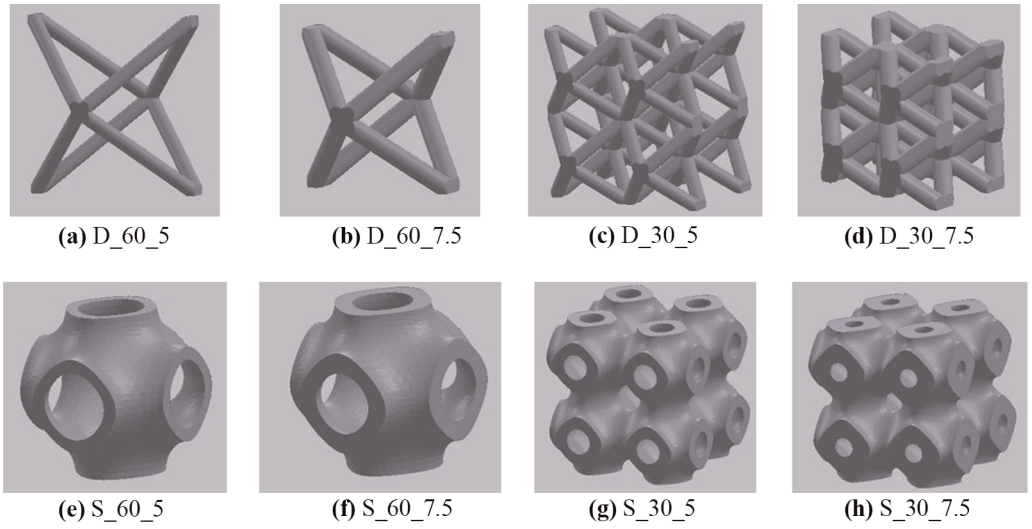

Figure 6 Negative design of the molds as a function of shape (D, S) function (CO, CA) cell dimension (30, 60) and node thickness (5)

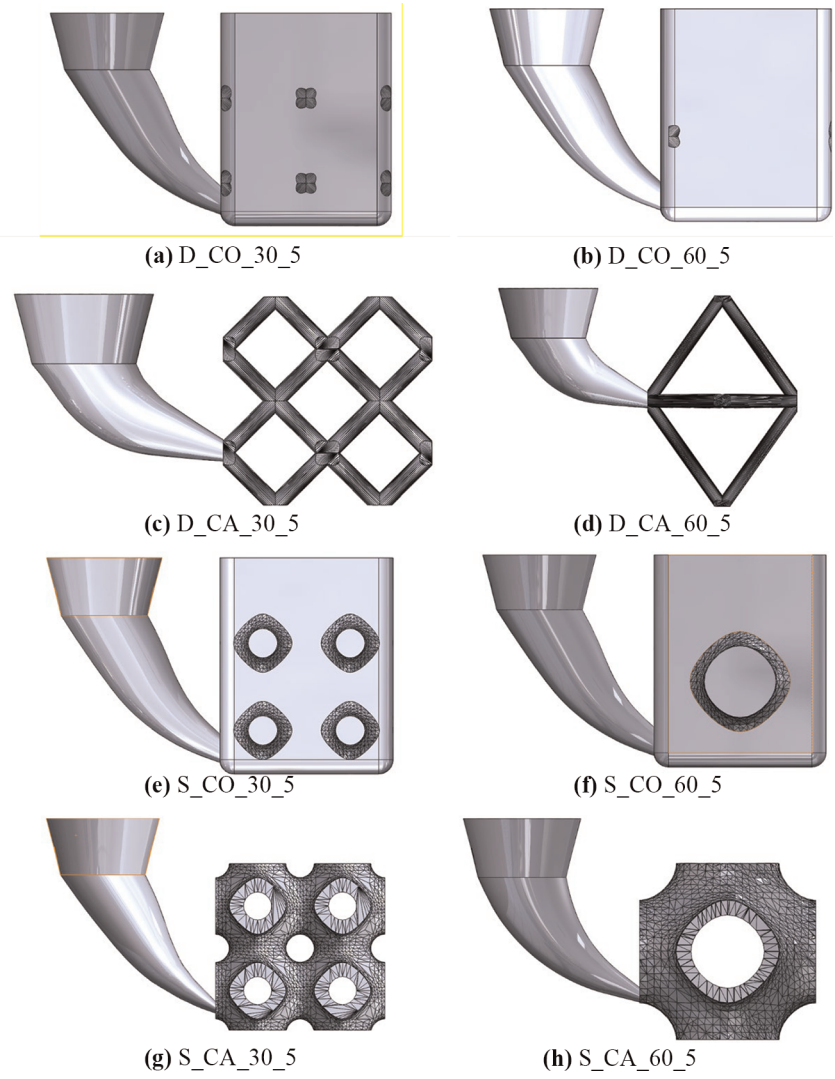

the pouring velocity v and gravity constant g is given by the formula:

$$H = \frac{v^2}{2g} \quad (1)$$

Cast and mold material, temperature and geometry have been set according to Tables 1, 2 and 3.

3. Results

3.1 Simple-part activity results

Figure 7(a) and 7(b) illustrate the cubes after 10 and 15 min of furnace treatment at 720°C. A darker color may be observed (during the test, fumes exited the muffle because of binder evaporation); however, all withstood the aluminum casting temperature. The fractures at the edges occurred during the handling of the cubes, when they were being taken out of the furnace. That the results of the SP.1 campaign indicate that the cube dimensions were not affected by the heat treatment.

The SP.2 campaign was subdivided into three parts: the gravity casting of aluminum into the open molds [Figure 8(a)], the cooling step, where a maintenance time of 15 min was implemented for the cube solidification (Figure 8b) and the cube extraction [Figure 8(c)]. The main results of the SP.2 campaign regarding the mold integrity for all tested geometries are the following: the molds with the thickness of 10–35 mm did not break during the test; on the contrary, cracks may be observed on the mold wall with a 5 mm wall thickness (Figure 9). However, cracks had been generated when the metal had already solidified; therefore, any defects on the cast surface were unnoticeable.

Figure 7 Set of cubes at the end of the SP.1 test

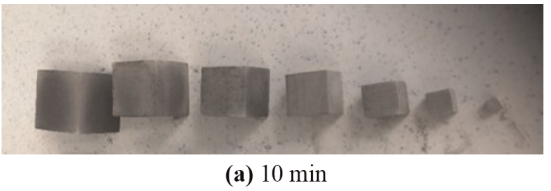

(a) 10 min

(b) 15 min

Figure 8 SP2 main steps: casting (a); cooling (b); and cube extraction (c)

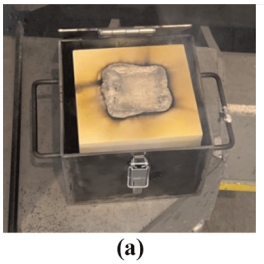

(a)

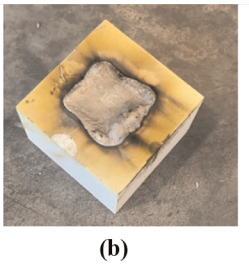

(b)

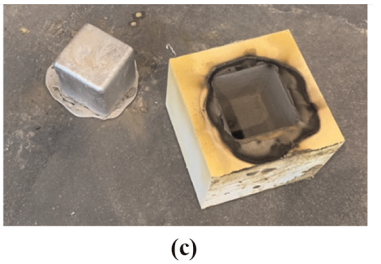

(c)

Figure 9 Crack formation during the cooling step of the mold with a 5 mm wall thickness

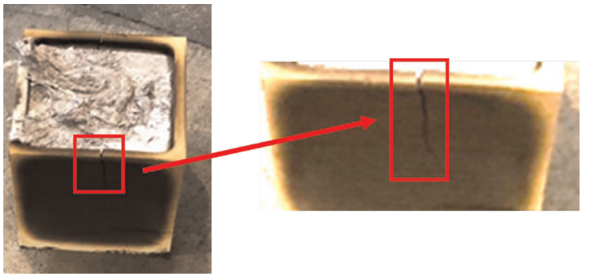

Figure 10 illustrates the cubes obtained after the extraction process; Table 6 lists the corresponding cross-section dimensions and average surface roughness.

Two main observations were made in this step. First, the dimensions and shape of the cubes indicated that all molds withstood the thermal stress caused by the casting and solidification phase; moreover, the roughness measured is lower that values typical of traditional sand casting (12 μm about). Second, several defects were observed at the bottom side owing to the presence of vaporized binder trapped during the solidification process and to the direct casting into the mold. However, despite the second observation, the simple part activity is successful because it demonstrates that the gypsum powder is able to withstand the casting temperature and the solidification of an aluminum alloy.

3.2 Complex-part activity results

The powder removal process of the designed internal channels was successful for most geometries, as summarized in Table 7; this is also the case for the thinnest channel diameter (5 mm).

As listed in Table 5, the powder could not be extracted for the case of the S-shape owing to the several changes in the direction, which resulted in a loss of pressure.

The results obtained from the CP.2 campaign are summarized in Figure 11, which shows the cast parts as a function of their geometry (Diamond – D or Schwarz P – S), cell dimension (60 or 30 mm), node thickness (5 or 7.5 mm) and function (cast – CA or core – CO). Based on the SP.2 results, where binder vaporization caused bubble defects, before casting, all molds had been pretreated in a furnace for 15 min at 150°C.

Figure 10 SP.2 results as a function of the mold thickness (bottom view)

Table 6 Section measures and surface roughness of the casted cubes

Mold thickness	35	30	25	20	15	10	5
X [mm]	59.53	59.61	59.84	59.74	59.87	59.97	60.03
Y [mm]	59.31	59.38	59.53	59.55	59.57	59.74	60.00
Ra [μm]	4.70	5.91	4.23	4.97	6.18	2.99	8.12

Table 7 CP.1 campaign results

		Channel diameter [mm]		
	Shape	5	7.5	10
2D	V	OK	OK	OK
	U	OK	OK	OK
	P	OK	OK	OK
	S	Failed	Failed	Failed
3D	V	OK	OK	OK
	U	OK	OK	OK
	P	OK	OK	OK
	S	Failed	Failed	Failed

In general, the entire set of molds withstood the casting and solidification step. The parts were extracted using water because of the solubility of the powder. However, as observed in the results illustrated in Figure 11, various defects were observed as a function of the tested geometry. The Diamond design [Figure 5(a) through 5(d)] that was used as cast generated a weak and breakable structure owing to crack generation and misruns during the solidification [Figures 11(a) through 11(c)]. Figure 11(d) is an exception, as the part was completed because of the higher node thickness (7.5 mm) and the smaller cell dimension (30 mm). On the contrary, parts generated using diamond as a core were successfully produced [Figure 5(e) through 5(h)]. No misrun defects were localized; meanwhile, porosity still existed. The parts obtained using the Schwarz P design [Figure 5(e) through 5(h)], either as a cast or a core, were successfully produced and the bubble-air defect was avoided. No significant differences were observed as a function of thickness; therefore, parts with a mold-cavity thickness of 5 mm [Figure 11(i) and 11(k)] could be filled. Misrun and skin porosity defects are evident in all cast geometries [Figure 11(i) through 11(l)] while core parts with cell dimension equal to 60 mm present and undesired base [Figure 11(m) and 11(n)] because of an error in the gating system design. Core parts obtained with 30 cell dimensions are correctly produced (Figure 11(o) and 11(p)].

Figure 12 shows the most significative simulation results as a function of the volume fraction.

Figure 12 display the volume fraction at the end of the filling step; as reported in Figure 12(f) red represents liquid material where there will be no filling issues on the contrary the multicolored areas could not fill completely and are, therefore, prone to shortage of material. The analysis highlights that core sample are still liquid and the end of filling [Figure 12(c)]. The Diamond geometries [Figure 12(a) and 12(b)] have critical issues related to their thin geometry that induce a solidification during the filling. The Schwarz P geometries [Figure 12(d) and 12(e)] presents similar problem but only focused on the outer edge. The comparison between Figure 12(b) and 12(f) demonstrates how an increase of node diameter increases the percentage of liquid material.

4. Discussion

The results of this preliminary study on the application of gypsum powder as a material for mold fabrication are summarized next:

- The SP.1 step indicated that gypsum parts produced via binder jetting could withstand the casting temperature of aluminum (720°C). This was confirmed by Figure 7, which showed that all specimens were still intact after the heat treatment. It is noteworthy that the binder evaporates during the test; thus, to control the binder is important to avoid porosity in the part during the casting process. Generally, it is better to pre heat the molds to reduce binder percentage as this makes it easier for the mold to be destroyed to remove the part. Moreover, as reported in Table 1, gypsum powder has a melting point of 1,400°C; thus, other materials such as magnesium, copper, gold, silver, zinc and their alloys can be used.
- The SP.2 step showed that molds with a wall thickness higher than 5 mm could resist aluminum casting. In fact, the entire set of specimens resisted in contact with the aluminum and fracture did not occur. Good results were also achieved for 5-mm thick molds because they started to crack only in the solidification phase and the dimensions of the generated part were coherent with the other parts produced (Table 5). This result is particularly important because it highlights the possibility of producing thin molds (at least 10 mm) that could conform to the casting shape to save material, thereby increasing process sustainability and decreasing mold cost. However, typical casting defects, such as porosity, were observed because of the gravity casting design that adds metal

Figure 11 CP.2 Campaign results: obtained cast complex parts

directly in the upper part of the mold; this prevents the vaporized binder from escaping. Moreover, the roughness measures highlight a better process performance of gypsum in term of surface quality respect to the traditional silica sand. The results founded are coherent with the results obtained by (Garzón *et al.*, 2017) and (Rodríguez-González *et al.*, 2020).

- The CP.1 step demonstrates the facility to remove the unbound powder from hollow parts. As shown in Table 6, most of the channels designed were emptied by the powder; this was also true when the diameter was 5 mm. This is a fundamental step because the feasibility to realize the void inside the mold by the powder removal process is the first step. The main constraint observed is the limitation of the removal process with respect to the air pressure in case of longer and more complex parts (S-shapes reported in Figure 3(d) and 3(h); however, other methods, such as the vacuum approach or designing an escape channel could be tested to increase the mold design complexity.
- The CP.2 step evaluates the capability of using the mold made by the gypsum powder to fabricate a complex part. A sprue and a riser were added into the cavity and the mold was pretreated to reduce the casting defects observed in the SP.2 step. Results show that all of the 16 molds tested resisted during the casting and the internal features did not collapse. At the end of the process, the parts could be easily extracted because most of the powder was unbound because of the binder vaporization. In particular it was observed that all the tests where the geometries designed (Figure 5) were used to generate the part core (CO) were completely produced; parts

Figure 12 Volume fraction analysis most significative results

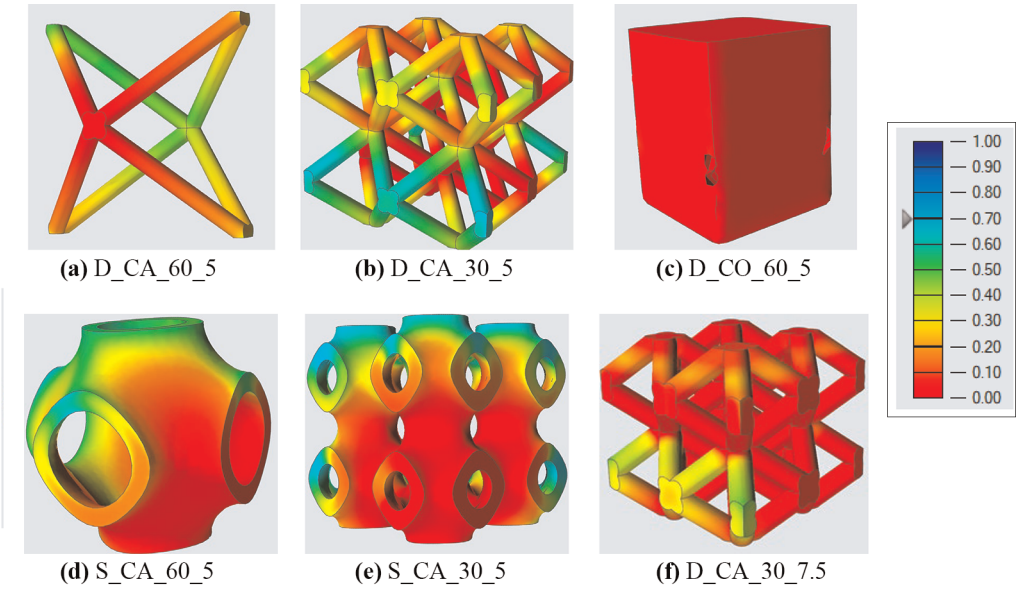

(a) D_CA_60_5 **(b)** D_CA_30_5 **(c)** D_CO_60_5

(d) S_CA_60_5 **(e)** S_CA_30_5 **(f)** D_CA_30_7.5

generated by lattice structure Schwarz – P give better results respect to Diamond because of their higher volume; cell dimension and node thickness not significantly affect the results. However, as Figure 11 shows, most of the parts obtained had different casting defects such as misrun, porosity and cold shuts. As the simulation confirmed a single gating system force the molten metal to divide it in different streams, in particular with all CA geometries having cell dimension equal to 30 mm, and this generates localized solidification phenomena during the filling step that leads to the misrun defect observed and generation of cold shuts. In particular in case of thinner parts as the D_CA_60_5 and D_CA_60_7.5 geometries to a fragmentation of the part itself. This fragmentation is coherent with the weakness measure from (Snelling *et al.*, 2015) and (Kim *et al.*, 2018) in case of the lattice structure demonstrators.

- However, the focus was on the gypsum resistance to complex part production, and the results confirm that its application in the sand casting process could be investigated.

4.1 Implication of research

The results found in this research improve the benefits related to AM application in industrial environment. As discussed in the introduction, process based on metallic powder deposition as SLM has limits in terms of production time, cost, part size, printable materials and part complexity: for these reasons, SLM founds limited application. The binder jetting technology with gypsum powder tested by the authors is able to solve most of the mentioned limits because it guarantees lower production time (hours vs days), lower machine cost (tens vs hundreds k€), higher printable volume (in binder jetting printers the parts are not attached on the build plate, so it is possible to print at different z position), more printable materials (theoretically all aluminum alloy con be cast inside gypsum mold) and in the CP2 step the authors demonstrated the possibility to produce complex part.

In particular foundry industries that use casting process with expendable mold and permanent pattern could test this technology that could guarantee a mold production avoiding all the problem related to pattern extraction, such as part division line, draft angle and undercuts. Moreover, benefits could be achieved also in case of casting process with expendable pattern such as investment casting because the economic benefits of these process are limited to mass production. The high costs and long lead-time associated with the development of hard tooling for wax pattern molding renders investment casting uneconomical for low-volume production; on the contrary binder jetting, as in general AM, because of their low set up times results more convenient.

5. Conclusion

In this study, the possibility of creating molds using gypsum binder jetting to cast complex geometry was evaluated. The main advantage is that complex parts can be fabricated, that is impossible to be produced via the sand casting process because of pattern extraction limits. Among the typically available binder jetting materials, the application of gypsum powder was tested because it could simplify the mold destruction step because of its water solubility and because owing to the powder size (27 μm) leads to parts with better surface roughness respect to sand casting. The preliminary tests showed that parts produced with this technology could withstand the aluminum casting temperature (720°C) and that there was no critical issue when the metal was poured into the 3D printed molds. Moreover, it was demonstrated that 5 mm thick features could satisfactorily withstand the aluminum pressure. The results also highlight some critical issues about mold cavity design in particular for the casting step. Generally, can be asserted that the results confirm the possibility to use gypsum powder in the aluminum casting process.

References

Almaghariz, E.S., Conner, B.P., Lenner, L., Gullapalli, R., Manogharan, G.P., Lamoncha, B. and Fang, M. (2016), "Quantifying the role of part design complexity in using 3d sand printing for molds and cores", *International Journal of Metalcasting*, Vol. 10 No. 3, pp. 240-252.

Bahnini, I., Rivette, M., Rechia, A., Siadat, A. and Elmesbahi, A. (2018), "Additive manufacturing technology: the status, applications, and prospects", *The International Journal of Advanced Manufacturing Technology*, Vol. 97 Nos 1/4, pp. 147-161.

Bai, Y. and Williams, C.B. (2018), "Binder jetting additive manufacturing with a particle-free metal ink as a binder precursor", *Materials & Design*, Vol. 147, pp. 146-156.

Bai, Y. and Williams, C.B. (2015), "An exploration of binder jetting of copper", *Rapid Prototyping Journal*, Vol. 21 No. 2, pp. 177-185.

Chhabra, M. and Singh, R. (2011), "Rapid casting solutions: a review", *Rapid Prototyping Journal*, Vol. 17 No. 5, pp. 328-350.

Dickens, P.M. (1995), "Research developments in rapid prototyping", *Proceedings of the Institution of Mechanical Engineers, Part B: Journal of Engineering Manufacture*, Vol. 209 No. 4, pp. 261-266.

Druschitz, A., Williams, C., Connelly, E. and Wood, B. (2017), *Advanced Castings Made Possible through Additive Manufacturing*, SAE Technical Papers.

Druschitz, A., Williams, C., Snelling, D. and Seals, M. (2014), "Additive manufacturing supports the production of complex castings", Paper presented at the TMS Annual Meeting, pp. 51-57.

Farzadi, A., Solati-Hashjin, M., Asadi-Eydivand, M. and Abu Osman, N.A. (2014), "Effect of layer thickness and printing orientation on mechanical properties and dimensional accuracy of 3D printed porous samples for bone tissue engineering", *PLoS ONE*, Vol. 9 No. 9, p. e108252.

Garzón, E.O., Alves, J.L. and Neto, R.J. (2017), "Study of the viability of manufacturing ceramic moulds by additive manufacturing for rapid casting", *Ciência & Tecnologia Dos Materiais*, Vol. 29 No. 1, pp. 275-280.

Gonzalez, J.A., Mireles, J., Lin, Y. and Wicker, R.B. (2016), "Characterization of ceramic components fabricated using binder jetting additive manufacturing technology", *Ceramics International*, Vol. 42 No. 9, pp. 10559-10564.

Hodder, K.J. and Chalaturnyk, R.J. (2019), "Bridging additive manufacturing and sand casting: utilizing foundry sand", *Additive Manufacturing*, Vol. 28, pp. 649-660.

Huang, G.-., Zhou, S. and Yuan, T. (2017), "Development of a wideband and high-efficiency waveguide-based compact antenna radiator with binder-jetting technique", *IEEE Transactions on Components, Packaging and Manufacturing Technology*, Vol. 7 No. 2, pp. 254-260.

Kang, J. and Ma, Q. (2017), "The role and impact of 3D printing technologies in casting", *China Foundry*, Vol. 14 No. 3, pp. 157-168.

Kim, D., Lee, J., Bae, J., Park, S., Choi, J., Lee, J.H. and Kim, E. (2018), "Mechanical analysis of ceramic/polymer composite with mesh-type lightweight design using binder-jet 3D printing", *Materials*, Vol. 11 No. 10, p. 11.

Kyogoku, H. (2018), "The current status and development of metal additive manufacturing technology", *Materia Japan*, Vol. 57 No. 4, pp. 140-144.

Le Néel, T.A., Mognol, P. and Hascoët, J.-Y. (2018a), "A review on additive manufacturing of sand molds by binder jetting and selective laser sintering", *Rapid Prototyping Journal*, Vol. 24 No. 8, pp. 1325-1336.

Le Néel, T.A., Mognol, P. and Hascoët, J.Y. (2018b), "Design methodology for variable shell mold thickness and thermal conductivity additively manufactured", *Welding in the World*, Vol. 62 No. 5, pp. 1059-1072.

Lores, A., Azurmendi, N., Agote, I. and Zuza, E. (2019), "A review on recent developments in binder jetting metal additive manufacturing: materials and process characteristics", *Powder Metallurgy*, Vol. 62 No. 5, pp. 267-296.

Lynch, P.C., Beniwal, C. and Wilck, J.H. IV. (2017), "Integration of binder jet additive manufacturing technology into the metal casting industry", Paper presented at the 67th Annual Conference and Expo of the Institute of Industrial Engineers 2017, pp. 1721-1726.

Mckenna, N., Singamneni, S., Diegel, O., Singh, D., Neitzert, T., George, J.S., Choudhury, A.R. and Yarlagadda, P. (2008), "Direct metal casting through 3D printing: a critical analysis of the mold characteristics", *9th Global Congress on Manufacturing and Management*, pp. 12-14.

Mitra, S., Rodríguez de Castro, A. and El Mansori, M. (2019), "On the rapid manufacturing process of functional 3D printed sand molds", *Journal of Manufacturing Processes*, Vol. 42, pp. 202-212.

Pham, D.T. and Gault, R.S. (1998), "A comparison of rapid prototyping technologies", *International Journal of Machine Tools and Manufacture*, Vol. 38 Nos 10/11, pp. 1257-1287.

Rodríguez-González, P., Fernández-Abia, A.I., Castro-Sastre, M.A. and Barreiro, J. (2020), "Heat treatments for improved quality binder jetted molds for casting aluminum alloys", *Additive Manufacturing*, Vol. 36, p. 101524.

Rooks, B. (2002), "Rapid tooling for casting prototypes", *Assembly Automation*, Vol. 22 No. 1, pp. 40-45.

Shangguan, H., Kang, J., Deng, C., Hu, Y. and Huang, T. (2017), "3D-printed shell-truss sand mold for aluminum castings", *Journal of Materials Processing Technology*, Vol. 250, pp. 247-253.

Shangguan, H., Kang, J., Yi, J., Zhang, X., Wang, X., Wang, H. and Huang, T. (2018), "The design of 3D-printed lattice-reinforced thickness-varying shell molds for castings", *Materials*, Vol. 11 No. 4, p. 11.

Sheydaeian, E. and Toyserkani, E. (2018), "Additive manufacturing functionally graded titanium structures with selective closed cell layout and controlled morphology", *The International Journal of Advanced Manufacturing Technology*, Vol. 96 Nos 9/12, pp. 3459-3469.

Snelling, D., Williams, C.B. and Druschitz, A.P. (2014), "A comparison of binder burnout and mechanical characteristics of printed and chemically bonded sand molds", *SFF Symp*, pp. 197-209.

Snelling, D., Li, Q., Meisel, N., Williams, C.B., Batra, R.C. and Druschitz, A.P. (2015), "Lightweight metal cellular structures fabricated via 3D printing of sand

cast molds", *Advanced Engineering Materials*, Vol. 17 No. 7, pp. 923-932.

Szymański, P. and Borowiak, M. (2019), "Evaluation of castings surface quality made in 3D printed sand moulds using 3DP technology", *Lecture Notes in Mechanical Engineering*, Vol. 4, pp. 201-212.

Walker, J., Harris, E., Lynagh, C., Beck, A., Lonardo, R., Vuksanovich, B. and MacDonald, E. (2018), "3D printed smart molds for sand casting", *International Journal of Metalcasting*, Vol. 12 No. 4, pp. 785-796.

Wang, J., Sama, S.R. and Manogharan, G. (2019), "Re-thinking design methodology for castings: 3D sand-printing and topology optimization", *International Journal of Metalcasting*, Vol. 13 No. 1, pp. 2-17.

Zhao, D., Guo, W., Zhang, B. and Gao, F. (2018), "3D sand mold printing: a review and a new approach", *Rapid Prototyping Journal*, Vol. 24 No. 2, pp. 285-300.

Ziaee, M. and Crane, N.B. (2019), "Binder jetting: a review of process, materials, and methods", *Additive Manufacturing*, Vol. 28, pp. 781-801.

Corresponding author

Luca Giorleo can be contacted at: luca.giorleo@unibs.it